Generalized effective-range expansion

S A Rakityansky[1,2] and N Elander[2]

[1] Department of Physics, University of Pretoria, Lynnwood Road, Pretoria 0002, South Africa
[2] Department of Physics, Stockholm University, Alba Nova University Center, Stockholm, SE-106 91, Sweden

Abstract

A systematic and accurate procedure has been developed for calculating the coefficients $\phi_{\ell n}^{(\text{in/out})}$ of the series expansion $f_\ell^{(\text{in/out})}(k) = \sum_{n=0}^\infty (k-k_0)^n \phi_{\ell n}^{(\text{in/out})}$ of the Jost functions in the vicinity of an arbitrary point k_0 in the complex momentum plane. This makes it possible to obtain an analytic expression for the S-matrix $s_\ell(k) = f_\ell^{(\text{out})}(k) / f_\ell^{(\text{in})}(k)$ around k_0 and locate its possible poles. In the particular case of $\ell = 0$ and $k_0 = 0$, any number of the parameters of the standard effective-range expansion $k \cot \delta_0 = -1/a + r_0 k^2/2 - \dots$ are easily obtained using the corresponding coefficients $\phi_{\ell n}^{(\text{in/out})}$. Numerical examples demonstrate the stability and accuracy of the proposed method.

PACS numbers: 03.65.Nk, 03.65.Ge, 24.30.Gd

1. Introduction

The effective-range theory was initially developed in nuclear physics when the details of low-energy nucleon–nucleon interaction were studied (see, for example, [1]). In the studies by Schwinger, Landau, Smorodinsky and Bethe (for a historical review, see, for example, [2]) it was shown that for a short-range potential the S-wave scattering phase shift δ_0 and the collision momentum k could be related as follows:

$$k \cot \delta_0 = -\frac{1}{a} + \frac{1}{2} r_0 k^2 - P r_0^3 k^4 + Q r_0^5 k^6 + \cdots, \tag{1}$$

where a, r_0, P, Q, etc are certain constants determined by the potential. The first two of these constants, namely, a and r_0, are known as the scattering length and the effective radius, respectively. The product $P r_0^3$ is sometimes called the scattering volume. The constants P, Q, etc are also collectively called the shape parameters. There was, however, no practical need to name the terms on the right-hand side of equation (1) beyond the first two because the procedure for calculating P, Q, etc was rather complicated and nobody actually took these higher terms into account.

A rather simple and regular procedure for calculating the terms of an expansion similar to (1) and its generalized version for a nonzero angular momentum, was developed on the basis

of the variable-phase method (see, for example, [3–6] and a review paper by Babikov [7]). This procedure had, however, a serious flaw: it broke down and required special regularization if the potential supported bound states. This drawback was overcome in the linear version of the variable-phase method [8, 9].

Nowadays the expansions of the type (1) are widely used not only in nuclear physics but also for parametrizing the low-energy collisions between atoms and molecules (see, for example, [10–15]).

In this paper, we describe the two main things. First, we derive simple first-order differential equations by solving which one can easily calculate any number of coefficients in the series expansion (1), and not only for the S-wave state, but also for any angular momentum $\ell \neq 0$. The proposed method is free from the singularities and does not need any regularization in the case of the potentials supporting bound states. Second, we generalize the expansion in such a way that it becomes a series of powers of $(k - k_0)$ with an arbitrary complex k_0. In other words, instead of making the expansion around the threshold point $k_0 = 0$, one can do it around any point in the complex plane. By doing this, one can, for example, explore the complex plane in search for resonances. Generally speaking, when $k_0 \neq 0$, the effective-range expansion is no longer a low-energy approximation.

2. Near-threshold expansion

Consider a particle of mass m moving in a central potential $U(r)$. To avoid any difficulties with the convergency of the power series expansions, we assume that this potential is of a short range, i.e. vanishes at large distances exponentially or faster, and is non-singular at the origin, i.e. is less singular than the centrifugal potential.

The radial wavefunction $u_\ell(k, r)$, corresponding to the angular momentum ℓ and the energy $E = (\hbar k)^2/(2m)$, is a solution of the Schrödinger equation

$$\left[\partial_r^2 + k^2 - \frac{\ell(\ell + 1)}{r^2} \right] u_\ell(k, r) = V(r) u_\ell(k, r), \tag{2}$$

where $V(r) = (2m/\hbar^2)U(r)$. As is shown in any textbook on quantum mechanics, with the above restrictions on the potential, a physical solution of this equation is regular at $r = 0$ and at short distances is proportional to the Riccati–Bessel function,

$$u_\ell(k, r) \underset{r \to 0}{\sim} j_\ell(kr). \tag{3}$$

The proportionality coefficient in equation (3) is an arbitrary constant that determines the wavefunction normalization. Since in our approach no observable quantities depend on the normalization, we can simply take this coefficient as unity.

2.1. Transformation of the Schrödinger equation

At large distances the right-hand side of equation (2) vanishes and therefore its solution becomes a linear combination of two linearly independent functions obeying the so-called 'free' Schrödinger equation

$$\left[\partial_r^2 + k^2 - \frac{\ell(\ell + 1)}{r^2} \right] u_\ell(k, r) = 0. \tag{4}$$

Thre are two possibilities for choosing such independent functions: either the Riccati–Bessel and Riccati–Neumann functions, $j_\ell(kr)$ and $n_\ell(kr)$, or the Riccatti–Hankel functions $h_\ell^{(\pm)}(kr)$, which are of course related to each other, namely,

$$h_\ell^{(\pm)}(kr) = j_\ell(kr) \pm i n_\ell(kr). \tag{5}$$

The idea is to look for the physical solution of equation (2) as either

$$u_\ell(k, r) = j_\ell(kr)A_\ell(k, r) - n_\ell(kr)B_\ell(k, r) \tag{6}$$

or

$$u_\ell(k, r) = h_\ell^{(-)}(kr)F_\ell^{(\text{in})}(k, r) + h_\ell^{(+)}(kr)F_\ell^{(\text{out})}(k, r) \tag{7}$$

not only at large distances, but everywhere on the segment $r \in [0, \infty)$. Of course, when $r \to \infty$, the functions $A_\ell(k, r)$ and $B_\ell(k, r)$, and similarly $F_\ell^{(\text{in/out})}(k, r)$, must converge to certain r-independent constants. In particular, the last two of them converge to the Jost functions,

$$F_\ell^{(\text{in})}(k, r) \xrightarrow[r \to \infty]{} f_\ell^{(\text{in})}(k), \tag{8}$$

$$F_\ell^{(\text{out})}(k, r) \xrightarrow[r \to \infty]{} f_\ell^{(\text{out})}(k), \tag{9}$$

which determine the S-matrix

$$s_\ell(k) = \frac{f_\ell^{(\text{out})}(k)}{f_\ell^{(\text{in})}(k)}. \tag{10}$$

By writing the ansatz (6) or (7), we introduce two unknown functions instead of just one function $u_\ell(k, r)$. This means that these two functions are not independent and therefore can be subjected to an arbitrary condition that relates them to each other. As such condition, it is convenient to choose either the equation

$$j_\ell(kr)\partial_r A_\ell(k, r) - n_\ell(kr)\partial_r B_\ell(k, r) = 0 \tag{11}$$

or similarly

$$h_\ell^{(-)}(kr)\partial_r F_\ell^{(\text{in})}(k, r) + h_\ell^{(+)}(kr)\partial_r F_\ell^{(\text{out})}(k, r) = 0. \tag{12}$$

This is a standard condition in the variation parameters method (which we are actually using here) for solving differential equations and is called the Lagrange condition (see, for example, [16]).

Substituting the ansatz (6) or (7) into equation (2) and using the Lagrange conditions (11) or (12) together with the known Wronskians $W_r[j_\ell(kr), n_\ell(kr)] = k$ and $W_r[h_\ell^{(-)}(kr), h_\ell^{(+)}(kr)] = 2ik$, we obtain the following systems of the first-order differential equations for the new unknown functions:

$$\partial_r A_\ell(k, r) = -\frac{1}{k}n_\ell(kr)V(r)[j_\ell(kr)A_\ell(k, r) - n_\ell(kr)B_\ell(k, r)], \tag{13}$$

$$\partial_r B_\ell(k, r) = -\frac{1}{k}j_\ell(kr)V(r)[j_\ell(kr)A_\ell(k, r) - n_\ell(kr)B_\ell(k, r)] \tag{14}$$

and

$$\partial_r F_\ell^{(\text{in})}(k, r) = -\frac{h_\ell^{(+)}(kr)}{2ik}V(r)[h_\ell^{(-)}(kr)F_\ell^{(\text{in})}(k, r) + h_\ell^{(+)}(kr)F_\ell^{(\text{out})}(k, r)], \tag{15}$$

$$\partial_r F_\ell^{(\text{out})}(k, r) = \frac{h_\ell^{(-)}(kr)}{2ik}V(r)[h_\ell^{(-)}(kr)F_\ell^{(\text{in})}(k, r) + h_\ell^{(+)}(kr)F_\ell^{(\text{out})}(k, r)]. \tag{16}$$

These systems are equivalent to each other and to equation (2), from which we started. The physical boundary conditions for them,

$$A_\ell(k, 0) = 1, \qquad B_\ell(k, 0) = 0 \tag{17}$$

and

$$F_\ell^{(\text{in})}(k, 0) = F_\ell^{(\text{out})}(k, 0) = 1/2, \tag{18}$$

follow immediately from equation (3).

2.2. Power series expansions

Our goal is to obtain a power series expansion of the type (1). To this end we recall the well-known series expansions of the Riccati–Bessel, Riccati–Neumann and Riccati–Hankel functions:

$$j_\ell(kr) = k^{\ell+1} \sum_{n=0}^{\infty} k^{2n} \gamma_{\ell n}(r), \tag{19}$$

$$n_\ell(kr) = k^{-\ell} \sum_{n=0}^{\infty} k^{2n} \eta_{\ell n}(r), \tag{20}$$

$$h_\ell^{(\pm)}(kr) = k^{-\ell} \sum_{n=0}^{\infty} k^{n} \chi_{\ell n}^{(\pm)}(r), \tag{21}$$

where the r-dependent coefficients $\gamma_{\ell n}(r)$, $\eta_{\ell n}(r)$ and $\chi_{\ell n}^{(\pm)}(r)$ are

$$\gamma_{\ell n}(r) = \frac{(-1)^n \sqrt{\pi}}{\Gamma\left(\ell + \frac{3}{2} + n\right) n!} \left(\frac{r}{2}\right)^{2n+\ell+1}, \tag{22}$$

$$\eta_{\ell n}(r) = \frac{(-1)^{n+\ell+1} \sqrt{\pi}}{\Gamma\left(-\ell + \frac{1}{2} + n\right) n!} \left(\frac{r}{2}\right)^{2n-\ell}, \tag{23}$$

$$\chi_{\ell n}^{(\pm)}(r) = \begin{cases} \pm i \eta_{\ell m}(r), & m = n/2 \quad \text{for even} \quad n \geqslant 0, \\ \gamma_{\ell m}(r), & m = (n - 2\ell - 1)/2 \quad \text{for odd} \quad n \geqslant 2\ell + 1, \\ 0, & \text{for odd} \quad n < 2\ell + 1. \end{cases} \tag{24}$$

2.2.1. Power series for $A_\ell(k, r)$ and $B_\ell(k, r)$.

We look for the functions $A_\ell(k, r)$ and $B_\ell(k, r)$ in the form of the power series similar to (19) and (20),

$$A_\ell(k, r) = k^a \sum_{n=0}^{\infty} k^{2n} \alpha_{\ell n}(r), \tag{25}$$

$$B_\ell(k, r) = k^b \sum_{n=0}^{\infty} k^{2n} \beta_{\ell n}(r), \tag{26}$$

where $a = 0$ because the boundary condition (17) can only be fulfilled if the leading term of the series (25) is k-independent. The power b in expansion (26) can be chosen in such a way that both terms on the right-hand side of equation (6) have the same power of the leading term, namely,

$$k^{\ell+1} k^0 = k^{-\ell} k^b \quad \Rightarrow \quad b = 2\ell + 1.$$

Therefore, our task now is to find a way of calculating the functions $\alpha_{\ell n}(r)$ and $\beta_{\ell n}(r)$ in the expansions

$$A_\ell(k, r) = \sum_{n=0}^{\infty} k^{2n} \alpha_{\ell n}(r), \tag{27}$$

$$B_\ell(k, r) = k^{2\ell+1} \sum_{n=0}^{\infty} k^{2n} \beta_{\ell n}(r). \tag{28}$$

This is achieved by substituting expansions (19), (20), (27) and (28) into the differential equations (13) and (14), and equating the terms of the same powers of k. As a result, we obtain the following system of differential equations for the functions $\alpha_{\ell n}(r)$ and $\beta_{\ell n}(r)$:

$$\partial_r \alpha_{\ell n} = - \sum_{i+j+m=n} \eta_{\ell i} V (\gamma_{\ell j} \alpha_{\ell m} - \eta_{\ell j} \beta_{\ell m}), \tag{29}$$

$$\partial_r \beta_{\ell n} = - \sum_{i+j+m=n} \gamma_{\ell i} V (\gamma_{\ell j} \alpha_{\ell m} - \eta_{\ell j} \beta_{\ell m}) \tag{30}$$

with the boundary conditions

$$\alpha_{\ell n}(0) = \delta_{n0}, \qquad \beta_{\ell n}(0) = 0, \qquad \forall \quad n = 0, 1, 2, \ldots. \tag{31}$$

2.2.2. Power series for $F_\ell^{(\text{in})}(k, r)$ and $F_\ell^{(\text{out})}(k, r)$. Using equations (5), the representation (6) of the radial wavefunction $u_\ell(k, r)$ can be transformed into the equivalent representation (7) and vice versa. In this way it is seen that

$$F_\ell^{(\text{in})}(k, r) = \frac{A_\ell(k, r) - \mathrm{i} B_\ell(k, r)}{2}, \tag{32}$$

$$F_\ell^{(\text{out})}(k, r) = \frac{A_\ell(k, r) + \mathrm{i} B_\ell(k, r)}{2}. \tag{33}$$

Therefore a series expansion for $F_\ell^{(\text{in/out})}(k, r)$ follows from the corresponding expansions (27, 28),

$$F_\ell^{(\text{in/out})}(k, r) = \frac{1}{2} \sum_{n=0}^{\infty} k^{2n} [\alpha_{\ell n}(r) \mp \mathrm{i} k^{2\ell+1} \beta_{\ell n}(r)]. \tag{34}$$

Similarly, the Jost functions,

$$f_\ell^{(\text{in/out})}(k) = \frac{1}{2} \sum_{n=0}^{\infty} k^{2n} [\alpha_{\ell n}(\infty) \mp \mathrm{i} k^{2\ell+1} \beta_{\ell n}(\infty)], \tag{35}$$

and the *S*-matrix (10) can be obtained as soon as the expansion coefficients $\alpha_{\ell n}$ and $\beta_{\ell n}$ are known. However, it is worthwhile to derive differential equations for direct calculation of the expansion coefficients $\phi_{\ell n}^{(\text{in/out})}(r)$ in the series representations

$$F_\ell^{(\text{in/out})}(k, r) = \sum_{n=0}^{\infty} k^n \phi_{\ell n}^{(\text{in/out})}(r). \tag{36}$$

This is done in the same way as we derived equations (29) and (30): by substituting expansions (21) and (36) into equations (15) and (16) and equating the coefficients of the same powers of the momentum. We thus obtain the differential equations

$$\partial_r \phi_{\ell n}^{(\text{in})} = -\frac{1}{2\mathrm{i}} \sum_{k+j+m=n+2\ell+1} \chi_{\ell k}^{(+)} V \big[\chi_{\ell j}^{(-)} \phi_{\ell m}^{(\text{in})} + \chi_{\ell j}^{(+)} \phi_{\ell m}^{(\text{out})} \big], \tag{37}$$

$$\partial_r \phi_{\ell n}^{(\text{out})} = \frac{1}{2\mathrm{i}} \sum_{k+j+m=n+2\ell+1} \chi_{\ell k}^{(-)} V \big[\chi_{\ell j}^{(-)} \phi_{\ell m}^{(\text{in})} + \chi_{\ell j}^{(+)} \phi_{\ell m}^{(\text{out})} \big], \tag{38}$$

with the boundary conditions

$$\phi_{\ell n}^{(\text{in})}(0) = \phi_{\ell n}^{(\text{out})}(0) = \tfrac{1}{2}\delta_{n0}. \tag{39}$$

Looking for zeros of $f_\ell^{(\text{in})}(k)$ at complex k, we can locate possible near-threshold bound states, resonances and virtual states. For example, a zero-energy bound state exists if $\alpha_{\ell 0}(\infty) = 0$ or equivalently $\phi_{\ell 0}^{(\text{in})}(\infty) = 0$.

2.3. Standard effective-range expansion

Recalling the asymptotic behavior of the Riccati–Bessel and Riccati–Neumann functions,

$$j_\ell(kr) \xrightarrow[|kr|\to\infty]{} \sin(kr - \ell\pi/2), \tag{40}$$

$$n_\ell(kr) \xrightarrow[|kr|\to\infty]{} -\cos(kr - \ell\pi/2), \tag{41}$$

we see that far away from the origin the wavefunction (6) takes the form

$$u_\ell(k, r) \xrightarrow[r\to\infty]{} \sin\left(kr - \frac{\ell\pi}{2}\right) A_\ell(k, \infty) + \cos\left(kr - \frac{\ell\pi}{2}\right) B_\ell(k, \infty). \tag{42}$$

On the other hand, the same asymptotics can be expressed via the scattering phase shift $\delta_\ell(k)$ as follows:

$$u_\ell(k, r) \xrightarrow[r\to\infty]{} N \sin\left(kr - \frac{\ell\pi}{2} + \delta_\ell\right), \tag{43}$$

where N is the normalization constant. Comparing equations (42) and (43), we see that

$$A_\ell(k, \infty) = N \cos\delta_\ell, \tag{44}$$

$$B_\ell(k, \infty) = N \sin\delta_\ell, \tag{45}$$

and therefore

$$\cot\delta_\ell = \frac{A_\ell(k, \infty)}{B_\ell(k, \infty)}. \tag{46}$$

With expansions (27) and (28), this gives the standard effective-range series

$$
\begin{aligned}
k^{2\ell+1}\cot\delta_\ell &= \frac{\alpha_{\ell 0}(\infty) + k^2\alpha_{\ell 1}(\infty) + k^4\alpha_{\ell 2}(\infty) + \cdots}{\beta_{\ell 0}(\infty) + k^2\beta_{\ell 1}(\infty) + k^4\beta_{\ell 2}(\infty) + \cdots} \\
&= \frac{\alpha_{\ell 0}(\infty)}{\beta_{\ell 0}(\infty)} + \left[\frac{\alpha_{\ell 1}(\infty)}{\beta_{\ell 0}(\infty)} - \frac{\alpha_{\ell 0}(\infty)\beta_{\ell 1}(\infty)}{\beta_{\ell 0}^2(\infty)}\right] k^2 \\
&\quad + \frac{\alpha_{\ell 0}(\infty)}{\beta_{\ell 0}(\infty)} \left\{\frac{\alpha_{\ell 2}(\infty)}{\alpha_{\ell 0}(\infty)} - \frac{\beta_{\ell 1}(\infty)}{\beta_{\ell 0}(\infty)}\left[\frac{\alpha_{\ell 1}(\infty)}{\alpha_{\ell 0}(\infty)} - \frac{\beta_{\ell 1}(\infty)}{\beta_{\ell 0}(\infty)}\right] - \frac{\beta_{\ell 2}(\infty)}{\beta_{\ell 0}(\infty)}\right\} k^4 \\
&\quad + O(k^6) + O(k^8) + \cdots.
\end{aligned}
\tag{47}
$$

In the case of $\ell = 0$, the terms on the right-hand side of this series are easily related to the scattering length, effective radius, scattering volume, etc, defined by equation (1). So, the procedure for calculating any number of terms in expansion (1) is very simple and can be made very accurate: starting from the initial values (31) at $r = 0$, we numerically solve the system of differential equations (29) and (30) outward up to a sufficiently large distance $r = R$ where the potential vanishes and the functions $\alpha_{\ell n}(r)$ and $\beta_{\ell n}(r)$ reach their asymptotic values $\alpha_{\ell n}(\infty)$ and $\beta_{\ell n}(\infty)$; the parameters of expansion (1) are then obtained by substituting these values into the corresponding terms of equation (47).

It should be noted that not all infinite number of equations in the system (29) and (30) are coupled to each other. Indeed, due to the condition $i + j + m = n$ on their right-hand sides, the equations for $\alpha_{\ell N}$ and $\beta_{\ell N}$ (for any $N \geqslant 0$) are only linked to the corresponding equations with $n < N$. For example, if we need just the scattering length, it is sufficient to solve only the following two equations:

$$\begin{cases} \partial_r \alpha_{00} = -\eta_{00} V (\gamma_{00} \alpha_{00} - \eta_{00} \beta_{00}), \\ \partial_r \beta_{00} = -\gamma_{00} V (\gamma_{00} \alpha_{00} - \eta_{00} \beta_{00}). \end{cases} \tag{48}$$

A calculation of the effective radius would require to add to the system the next pair of equations, and so on. Similarly, the system of differential equations (37), (38) do not have to be truncated when we need only first N coefficients $\phi_{\ell n}^{(\text{in/out})}$, $n = 1, 2, \ldots, N$.

3. Expansion near an arbitrary point

Since the Jost function is analytic on the whole k-plane, it can be uniquely represented by a convergent power series at any point on that plane. Apparently, this is also true for the functions $F_{\ell}^{(\text{in/out})}$ as well as for A_{ℓ} and B_{ℓ}. In order to obtain such expansions for these functions, we generalize the series (19)–(21) as follows:

$$j_{\ell}(kr) = k^{\ell+1} \sum_{n=0}^{\infty} (k - k_0)^n \tilde{\gamma}_{\ell n}(k_0, r), \tag{49}$$

$$n_{\ell}(kr) = k^{-\ell} \sum_{n=0}^{\infty} (k - k_0)^n \tilde{\eta}_{\ell n}(k_0, r), \tag{50}$$

$$h_{\ell}^{(\pm)}(kr) = k^{-\ell} \sum_{n=0}^{\infty} (k - k_0)^n \tilde{\chi}_{\ell n}^{(\pm)}(k_0, r). \tag{51}$$

Here the functions $\tilde{\gamma}_{\ell n}(k_0, r)$, $\tilde{\eta}_{\ell n}(k_0, r)$ and $\tilde{\chi}_{\ell n}^{(\pm)}(k_0, r)$ differ from (22), (23) and (24), respectively. Generally, they are non-zero for any n (odd or even) and depend on the point k_0 around which the expansion is done,

$$\tilde{\gamma}_{\ell n}(k_0, r) = \frac{1}{n!} \left\{ \frac{\mathrm{d}^n}{\mathrm{d}k^n} \left[\frac{j_{\ell}(kr)}{k^{\ell+1}} \right] \right\} \bigg|_{k=k_0}, \tag{52}$$

$$\tilde{\eta}_{\ell n}(k_0, r) = \frac{1}{n!} \left\{ \frac{\mathrm{d}^n}{\mathrm{d}k^n} [n_{\ell}(kr) k^{\ell}] \right\} \bigg|_{k=k_0}, \tag{53}$$

$$\tilde{\chi}_{\ell n}^{(\pm)}(k_0, r) = \frac{1}{n!} \left\{ \frac{\mathrm{d}^n}{\mathrm{d}k^n} \left[h_{\ell}^{(\pm)}(kr) k^{\ell} \right] \right\} \bigg|_{k=k_0}. \tag{54}$$

Of course, these functions coincide with the corresponding coefficients (22), (23) and (24) when $k_0 = 0$ (the odd-order derivatives (52) and (53) vanish at $k = 0$ and thus only the even-power terms in the series (49) and (50) remain).

A recurrent procedure for calculating the expansion coefficients (52)–(54) can be developed using the following formulae (see, for example, [19]):

$$\left(\frac{1}{z} \frac{\mathrm{d}}{\mathrm{d}z} \right)^n \frac{j_{\ell}(z)}{z^{\ell+1}} = (-1)^n \frac{j_{\ell+n}(z)}{z^{\ell+n+1}}, \tag{55}$$

$$\left(\frac{1}{z}\frac{\mathrm{d}}{\mathrm{d}z}\right)^n [z^\ell x_\ell(z)] = z^{\ell-n} x_{\ell-n}(z), \tag{56}$$

where $x_\ell(z)$ stands for either of the functions $h_\ell^{(\pm)}(z)$ or $n_\ell(z)$.

3.1. Power series for $A_\ell(k, r)$ and $B_\ell(k, r)$

Similar to equations (27) and (28), we look for A_ℓ and B_ℓ as

$$A_\ell(k, r) = \sum_{n=0}^\infty (k - k_0)^n \tilde\alpha_{\ell n}(k_0, r), \tag{57}$$

$$B_\ell(k, r) = k^{2\ell+1} \sum_{n=0}^\infty (k - k_0)^n \tilde\beta_{\ell n}(k_0, r). \tag{58}$$

Substituting expansions (49), (50), (57) and (58) into equations (13) and (14), and equating the coefficients of the same powers of $(k - k_0)$, we obtain the differential equations,

$$\partial_r \tilde\alpha_{\ell n} = - \sum_{i+j+m=n} \tilde\eta_{\ell i} V(\tilde\gamma_{\ell j}\tilde\alpha_{\ell m} - \tilde\eta_{\ell j}\tilde\beta_{\ell m}), \tag{59}$$

$$\partial_r \tilde\beta_{\ell n} = - \sum_{i+j+m=n} \tilde\gamma_{\ell i} V(\tilde\gamma_{\ell j}\tilde\alpha_{\ell m} - \tilde\eta_{\ell j}\tilde\beta_{\ell m}), \tag{60}$$

which look exactly like the corresponding equations for the functions $\alpha_{\ell n}(r)$ and $\beta_{\ell n}(r)$. The boundary conditions also remain the same,

$$\tilde\alpha_{\ell n}(k_0, 0) = \delta_{n0}, \qquad \tilde\beta_{\ell n}(k_0, 0) = 0, \qquad \forall \quad n = 0, 1, 2, \ldots. \tag{61}$$

The expansion for the Jost functions around an arbitrary point k_0 takes the form

$$f_\ell^{(\mathrm{in/out})}(k) = \frac{1}{2} \sum_{n=0}^\infty (k - k_0)^n [\tilde\alpha_{\ell n}(k_0, \infty) \mp \mathrm{i}k^{2\ell+1}\tilde\beta_{\ell n}(k_0, \infty)]. \tag{62}$$

It should be noted that, in contrast to equation (35), it involves all powers of $(k - k_0)$. It is not difficult to check that when $k_0 \to 0$, the odd coefficients in the series (57) and (58) vanish because of the zero boundary conditions (61) for the corresponding differential equations which only remain linked to the other equations with the odd numbers.

3.2. Effective range expansion near an arbitrary point

Equations (57) and (58) give just another representation of the same functions $A_\ell(k, r)$ and $B_\ell(k, r)$ as do the corresponding equations (27) and (28). We therefore can repeat all the steps of section 2.3 and derive a similar equation:

$$k^{2\ell+1} \cot\delta_\ell = \frac{\sum_{n=0}^\infty (k - k_0)^n \tilde\alpha_{\ell n}(k_0, \infty)}{\sum_{n=0}^\infty (k - k_0)^n \tilde\beta_{\ell n}(k_0, \infty)}, \tag{63}$$

where, in contrast to equation (47), all powers (odd and even) of $(k - k_0)$ are present. In the case of $\ell = 0$ we can introduce the scattering length $\tilde a(k_0)$ with respect to the momentum k_0,

$$\tilde a(k_0) = -\frac{\tilde\beta_{00}(k_0, \infty)}{\tilde\alpha_{00}(k_0, \infty)}, \tag{64}$$

and the other shape parameters as the coefficients of the series

$$k \cot\delta_0 = -\frac{1}{\tilde a(k_0)} + \tilde b(k_0)(k - k_0) + \frac{1}{2}\tilde r_0(k_0)(k - k_0)^2 + \cdots. \tag{65}$$

These coefficients can be obtained by dividing two polynomials in equation (63).

3.3. Power series for $F_\ell^{(\mathrm{in})}(k,r)$ and $F_\ell^{(\mathrm{out})}(k,r)$

Let us look for $F_\ell^{(\mathrm{in/out})}(k,r)$ in the form of the following power series:

$$F_\ell^{(\mathrm{in/out})}(k,r) = \sum_{n=0}^{\infty}(k-k_0)^n \tilde\phi_{\ell n}^{(\mathrm{in/out})}(k_0,r). \tag{66}$$

Substituting it into equations (15) and (16) together with expansions (51) give

$$k^{2\ell+1}\sum_{n=0}^{\infty}(k-k_0)^n \partial_r\tilde\phi_{\ell n}^{(\mathrm{in/out})} = \mp\frac{1}{2\mathrm{i}}\sum_{ijm}(k-k_0)^{i+j+m}\tilde\chi_{\ell i}^{(\pm)}V\left[\tilde\chi_{\ell j}^{(-)}\tilde\phi_{\ell m}^{(\mathrm{in})}+\tilde\chi_{\ell j}^{(+)}\tilde\phi_{\ell m}^{(\mathrm{out})}\right]. \tag{67}$$

In order to equate the coefficients of the same powers of $(k-k_0)$ the factor $k^{2\ell+1}$ on the left-hand side can be transformed as

$$k^{2\ell+1} = (k-k_0+k_0)^{2\ell+1} = \sum_{j=0}^{2\ell+1}\binom{2\ell+1}{j}(k-k_0)^{2\ell+1-j}k_0^j,$$

where

$$\binom{m}{n} = \frac{m!}{n!(m-n)!}$$

are the binomial coefficients. For the left-hand side of equation (67), we therefore have

$$\sum_{m=0}^{\infty}\sum_{j=0}^{2\ell+1}(k-k_0)^{2\ell+1+m-j}\binom{2\ell+1}{j}k_0^j\partial_r\tilde\phi_{\ell m}^{(\mathrm{in/out})}$$

$$= \sum_{n=0}^{\infty}(k-k_0)^n\sum_{j=0}^{2\ell+1}\binom{2\ell+1}{j}k_0^j\partial_r\tilde\phi_{\ell,n+j-2\ell-1}^{(\mathrm{in/out})},$$

where it is assumed that $\tilde\phi_{\ell,n}^{(\mathrm{in/out})}\equiv 0\,\forall\,n<0$. In this form it is easy to compare the left- and right-hand sides of equation (67) and thus to obtain the equations that we were aimed to

$$\sum_{j=0}^{2\ell+1}\binom{2\ell+1}{j}k_0^j\partial_r\tilde\phi_{\ell,n+j-2\ell-1}^{(\mathrm{in})} = -\frac{1}{2\mathrm{i}}\sum_{i+j+m=n}\tilde\chi_{\ell i}^{(+)}V\left[\tilde\chi_{\ell j}^{(-)}\tilde\phi_{\ell m}^{(\mathrm{in})}+\tilde\chi_{\ell j}^{(+)}\tilde\phi_{\ell m}^{(\mathrm{out})}\right], \tag{68}$$

$$\sum_{j=0}^{2\ell+1}\binom{2\ell+1}{j}k_0^j\partial_r\tilde\phi_{\ell,n+j-2\ell-1}^{(\mathrm{out})} = \frac{1}{2\mathrm{i}}\sum_{i+j+m=n}\tilde\chi_{\ell i}^{(-)}V\left[\tilde\chi_{\ell j}^{(-)}\tilde\phi_{\ell m}^{(\mathrm{in})}+\tilde\chi_{\ell j}^{(+)}\tilde\phi_{\ell m}^{(\mathrm{out})}\right], \tag{69}$$

where $n=0,1,2,\ldots$. The boundary conditions are the same as given by equation (39),

$$\tilde\phi_{\ell n}^{(\mathrm{in})}(k_0,0) = \tilde\phi_{\ell n}^{(\mathrm{out})}(k_0,0) = \tfrac{1}{2}\delta_{n0}. \tag{70}$$

Similar to all other infinite systems of equations derived in this paper, not all of these equations are linked. For any $N\geqslant 0$, the first N pairs of them ($n=0,1,2,\ldots,N$) are selfcontained and can be solved independently of the rest of the system. In other words, every next pair of equations is linked to all equations with lower n, but not the other way round.
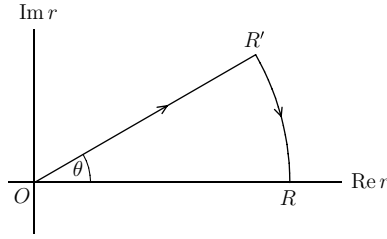
Figure 1. A deformed path for integrating the differential equations.

4. Complex rotation

At a first sight, it may seem that equations (59) and (60), or equivalent equations (68) and (69), allow us to obtain an analytic (polynomial) approximation of the Jost functions and thus the S-matrix near any chosen point k_0 in the complex k-plane. However, this is only partially true. They indeed work very well for any point k_0 on the real axis and thus allow us to calculate the Jost functions for complex k within the domain of validity of expansions (62) or (66) around the point k_0. However, if we move k_0 itself into the complex momentum plane the solutions of these differential equations diverge at large distances.

The reason for this divergence lies in the fact that one of the functions $h_\ell^{(\pm)}(kr)$ is always divergent if $\mathrm{Im}\, k \neq 0$,

$$h_\ell^{(+)}(kr) \xrightarrow[r\to\infty]{} \infty, \qquad \text{for} \quad \mathrm{Im}\, k < 0, \tag{71}$$

$$h_\ell^{(-)}(kr) \xrightarrow[r\to\infty]{} \infty, \qquad \text{for} \quad \mathrm{Im}\, k > 0. \tag{72}$$

Both $j_\ell(kr)$ and $n_\ell(kr)$ are linear combinations of $h_\ell^{(\pm)}(kr)$ and therefore also exponentially diverge when $\mathrm{Im}\, k \neq 0$, which makes divergent the expansion coefficients (52) and (53) as well as the solutions of equations (59) and (60). Apparently, the same is true for the expansion coefficients (54) and thus for the solutions of equations (68) and (69).

There is a way to circumvent this problem. The trick consists in using a complex rotation of the coordinate. Indeed, what we actually need are the limits

$$\tilde{\alpha}_{\ell n}(k_0, \infty) = \lim_{r\to\infty} \tilde{\alpha}_{\ell n}(k_0, r), \tag{73}$$

$$\tilde{\beta}_{\ell n}(k_0, \infty) = \lim_{r\to\infty} \tilde{\beta}_{\ell n}(k_0, r), \tag{74}$$

$$\tilde{\phi}_{\ell n}^{(\mathrm{in/out})}(k_0, \infty) = \lim_{r\to\infty} \tilde{\phi}_{\ell n}^{(\mathrm{in/out})}(k_0, r), \tag{75}$$

which are reached at a sufficiently large $r = R$ (where the potential vanishes). We can obtain these limits by integrating the corresponding differential equations either along the real axis (see figure 1) from O to R, or making a detour ($O \to R' \to R$) into the complex plane. On the faraway arc $R' \to R$, however, the solutions do not change because the potential vanishes. This means that in order to get the limits (73)–(75) it is sufficient to reach the point R' instead of R.

In other words, in our differential equations, the real variable r can be replaced with a complex one,

$$r = \rho\, \mathrm{e}^{\mathrm{i}\theta}. \tag{76}$$

How to choose the rotation angle θ? The purpose of the rotation is to avoid the divergences (71) and (72), which is possible if $\mathrm{Im}(k_0 r) = 0$ on the integration path. The product $k_0 r$ is real if

$$\theta = -\arctan\left(\frac{\mathrm{Im}\, k_0}{\mathrm{Re}\, k_0}\right). \tag{77}$$

Of course, we can only do the rotation if the potential allows us to do so, i.e. if it is analytic and vanishes at infinity along the ray (76). Actually, it is sufficient if the potential has an analytic tail. Indeed, we can always appropriately modify the integration path in such a way that we move along the real axis until it is safe to turn into the complex plane and on the ray (76).

5. Constructing potentials with given properties

It often happens that one needs to construct a potential that describes given experimental data. The approach proposed in this paper could be useful in adjusting the potential in such a way that it generates a resonance pole of the S-matrix at a given point of the complex k-plane.

As was already mentioned at the end of section 2.2.2, the S-matrix has a pole exactly at $k = 0$ if $\phi_{\ell 0}^{(\mathrm{in})}(\infty) = 0$. Looking at equation (66), we see that, similarly to $k = 0$, the S-matrix has a pole at any given complex point k_0 if

$$\tilde{\phi}_{\ell 0}^{(\mathrm{in})}(k_0, \infty) = 0. \tag{78}$$

One therefore only needs to solve the simple system of two differential equations

$$k_0^{2\ell+1} \partial_r \tilde{\phi}_{\ell 0}^{(\mathrm{in})} = -\frac{1}{2\mathrm{i}} \tilde{\chi}_{\ell 0}^{(+)} V\left[\tilde{\chi}_{\ell 0}^{(-)} \tilde{\phi}_{\ell 0}^{(\mathrm{in})} + \tilde{\chi}_{\ell 0}^{(+)} \tilde{\phi}_{\ell 0}^{(\mathrm{out})}\right], \tag{79}$$

$$k_0^{2\ell+1} \partial_r \tilde{\phi}_{\ell 0}^{(\mathrm{out})} = \frac{1}{2\mathrm{i}} \tilde{\chi}_{\ell 0}^{(-)} V\left[\tilde{\chi}_{\ell 0}^{(-)} \tilde{\phi}_{\ell 0}^{(\mathrm{in})} + \tilde{\chi}_{\ell 0}^{(+)} \tilde{\phi}_{\ell 0}^{(\mathrm{out})}\right], \tag{80}$$

which follow from equations (68) and (69) when $n = 0$, and vary the parameters of the potential until the condition (78) is achieved. Of course, equations (79) and (80) should be solved along the complex path as is described in the previous section.

6. Numerical examples

In order to examine how the suggested method works, we did numerical calculations for well-studied potentials. Since in our method there is nothing special concerning the angular momentum, we only tested the case $\ell = 0$.

6.1. Testing the accuracy of the expansions

The first example is an exponential hump, shown in figure 2. It is positive everywhere and therefore can only support resonant states. In the units such that $\hbar = m = 1$, the functional form of this potential is

$$V(r) = 7.5r^2 \exp(-r). \tag{81}$$

The exact S-matrix corresponding to this potential has an infinite number of poles forming a string that goes down the k-plane to infinity. The exact locations of the first four of these poles are given in table 1. These values of the resonance energies were obtained using a very accurate method, which is based on a combination of the complex rotation and a direct calculation of the Jost function (see [18]).
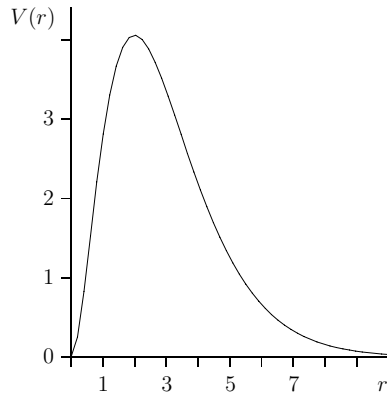
Figure 2. Testing potential (81) in the arbitrary units such that $\hbar = m = 1$.

Table 1. The first four S-wave resonance points, $k^2/(2m) = E_{\mathrm{r}} - \mathrm{i}\Gamma/2$, of the exact S-matrix for the potential (81). All the values are given in the arbitrary units such that $\hbar = m = 1$. They were obtained using the Jost function method described in [18].

Re k	Im k	E_{r}	Γ
2.617 786 1703	−0.004 879 8793	3.426 390 3101	0.025 548 9612
3.130 042 4437	−0.357 144 2525	4.834 806 8411	2.235 753 3377
3.398 392 4252	−0.997 251 8977	5.277 279 8640	6.778 106 5905
3.591 463 0921	−1.663 955 5063	5.064 929 6074	11.952 069 5757

6.1.1. Real axis. To begin with, we tested how our expansion works when k is on the real axis. For this, we compared the S-wave scattering phase shift obtained using five terms of the series (57) and (58), with the exact phase shift. The results for the expansions around the points $k_0 = 0, 1, 2, 3$ are shown in figures 3–6. It is seen that even with only five terms the expansion reproduces δ_0 within a reasonably wide range of the momentum around the point k_0.

6.1.2. Complex momenta. The Jost function is an analytic function of k. Therefore if we accurately approximate it with a polynomial on the real axis, this polynomial must be able to reproduce it at the nearby complex points as well. To examine the accuracy, we calculated the S-wave S-matrix,

$$s_0(k) = \frac{\sum_{n=0}^{N}(k - k_0)^n \tilde{\phi}_{0n}^{(\mathrm{out})}(k_0, \infty)}{\sum_{n=0}^{N}(k - k_0)^n \tilde{\phi}_{0n}^{(\mathrm{in})}(k_0, \infty)}, \tag{82}$$

and compared it with the exact one. Moving from k_0 along a straight line, we stop at a point where the error exceeds certain value ε. Checking in this way all the directions around k_0, we obtain a closed curve that bounds a domain within which the error is less than ε.

Figure 7 shows the accuracy domains for $\varepsilon = 1\%$, 5% and 10% around each of the three points $k_0 = 2, 2.5$ and $2.5 - \mathrm{i}0.5$. These domains were obtained with only five terms in the Jost function expansions. When we increased the number of terms N in expansions (82) from $N = 5$ to $N = 15$, the accuracy domain widens. For the case of $\varepsilon = 1\%$, it is shown in figure 8.
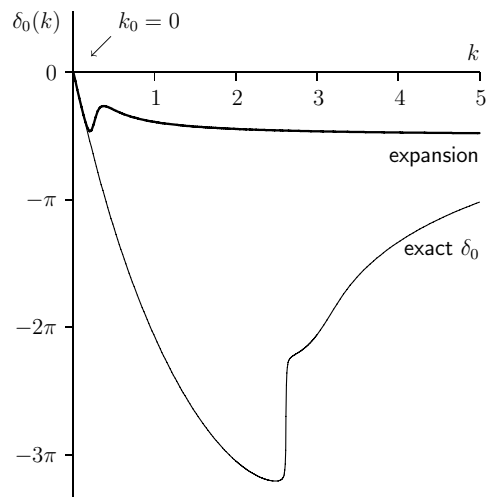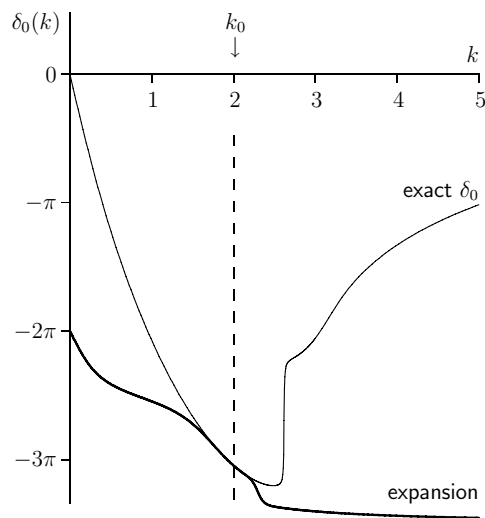
Figure 3. The exact *S*-wave scattering phase shift for the potential (81) is compared with the corresponding phase shift obtained using the first five terms of expansions (57) and (58) at $k_0 = 0$.
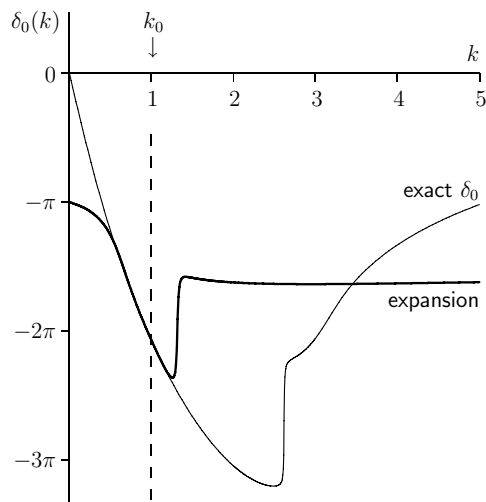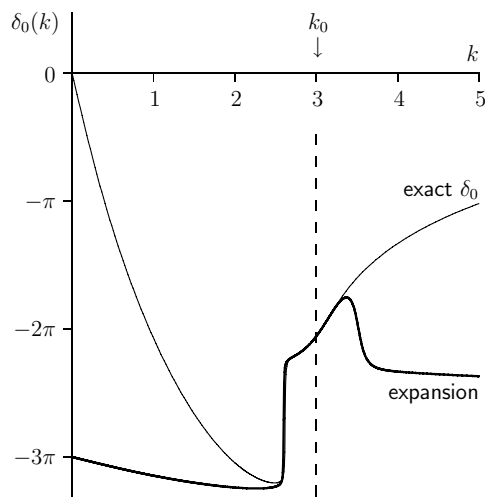

Figure 4. The exact *S*-wave scattering phase shift for the potential (81) is compared with the corresponding phase shift obtained using the first five terms of expansions (57) and (58) at $k_0 = 1$.

Since our polynomial reproduces the Jost function in a certain domain of the complex *k*-plane, it should have (within this domain) the same zeros (if any) as the exact Jost function. But a polynomial always has zeros and the number of them is equal to its order. These means that some (or all) of its zeros are spurious and do not correspond to resonances. In figure 9, all 25 zeros of the polynomial approximation

$$f_0^{(in)}(k) = \sum_{n=0}^{N} (k - k_0)^n \tilde{\phi}_{0n}^{(in)}(k_0, \infty)$$

13

Figure 5. The exact *S*-wave scattering phase-shift for the potential (81) is compared with the corresponding phase-shift obtained using the first five terms of expansions (57) and (58) at $k_0 = 2$.


Figure 6. The exact *S*-wave scattering phase shift for the potential (81) is compared with the corresponding phase shift obtained using the first five terms of expansions (57) and (58) at $k_0 = 3$.

with $N = 25$ are shown for the expansion around $k_0 = 2.9 - i0.18$, which is in between of two resonances. It is seen that two zeros coincide with the resonances, which are within the 1% accuracy domain, while the other zeros are spurious. If we change N, the true zeros remain at their places, while the spurious ones move unpredictably (but always outside the 1% accuracy domain).

14
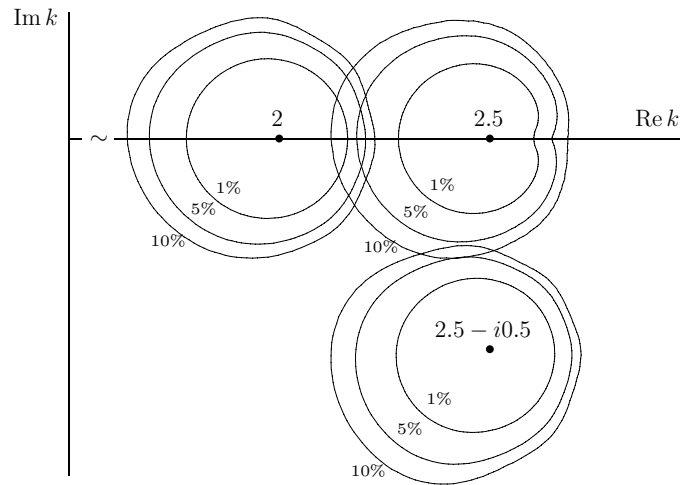
Figure 7. The domains of the complex k-plane, within which the S-wave S-matrix for the potential (81) is reproduced, using the first five terms of expansions (66), with the accuracy better than 1%, 5% and 10%. The dots show the corresponding values of k_0, around which the expansions were done.
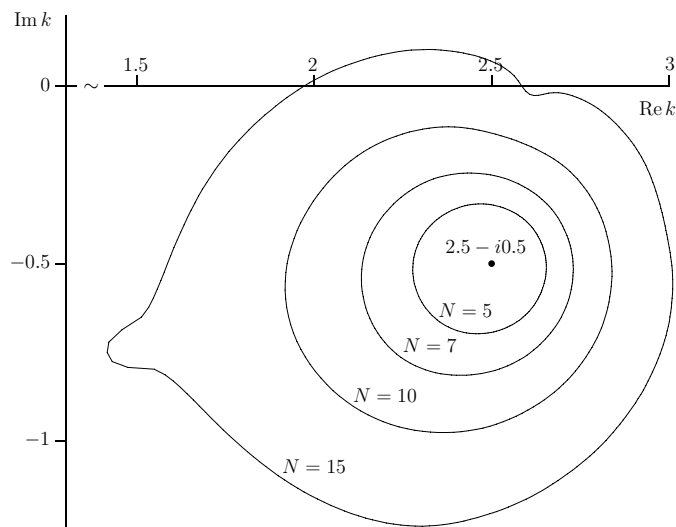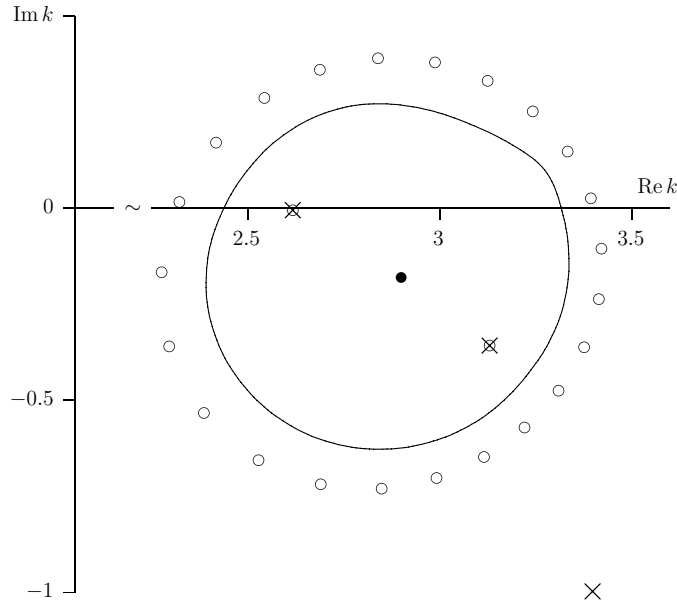

Figure 8. Growth of the 1% accuracy domain with the increase of the number N of terms in expansions (66), which were done around $k_0 = 2.5 - \mathrm{i}0.5$ for the S-wave scattering from the potential (81).

6.2. Locating virtual states

As an example of the potential generating a virtual state, we chose the singlet nucleon–nucleon interaction,

$$V_{\mathrm{NN}}(r) = -W \exp(-r/\rho), \tag{83}$$

15

Figure 9. Zeros (open circles) of the polynomial $f_0^{(\text{in})}(k) = \sum_{n=0}^{N}(k-k_0)^n \tilde{\phi}_{0n}^{(\text{in})}(k_0, \infty)$ for $N = 25$ and $k_0 = 2.9 - i0.18$ (shown by the filled circle). The closed curve shows the domain within which the exact Jost function is reproduced by this polynomial with the accuracy better than 1%. Crosses show the first three *S*-wave resonances generated by the potential (81).

Table 2. Convergence of the nucleon–nucleon virtual state located using N terms of expansion (35). Its position on the complex k-plane is shown in figure 10.

N	k fm^{-1}	$E = \hbar^2 k^2/(2\mu)$ MeV
0	$-i0.042\,118\,4878$	$-0.073\,566\,4122$
1	$-i0.039\,919\,4293$	$-0.066\,084\,9678$
2	$-i0.039\,913\,2589$	$-0.066\,064\,5396$
3	$-i0.039\,913\,2384$	$-0.066\,064\,4717$
4	$-i0.039\,913\,2383$	$-0.066\,064\,4715$
Exact	$-i0.039\,913\,2383$	$-0.066\,064\,4715$

where $W = 104.20$ MeV and $\rho = 0.73$ fm. With $\hbar^2/(2\mu) = 41.47$ Mev fm^2, its virtual state is at $k = -i0.039\,913\,2383$ fm^{-1} and $E = \hbar^2 k^2/(2\mu) = -0.066\,064\,4715$ Mev (see, for example, [20]). Calculating the expansion coefficients of equation (35), we located the Jost function zeros for an increasing number of terms in the expansion. Table 2 shows a rapid convergence of the pole we thus found on the imaginary axis, to its true position. In figure 10, all nine zeros of the polynomially approximated Jost function (for four terms in the expansion) are shown. In addition to the true zero, the polynomial has many spurious zeros, which change their positions when the number of terms is changed.

6.3. Putting a resonance pole at a given place

In order to demonstrate the ability of the proposed method, we adjusted (as described in section 5) the height and width of the potential barrier (81) in such a way that its first
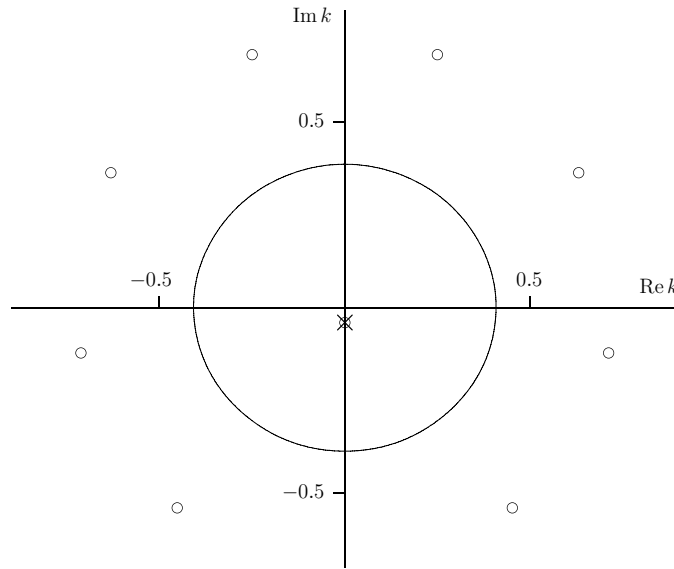
Figure 10. Zeros (open circles) of the polynomial $f_0^{(in)}(k) = \sum_{n=0}^{N}(k - k_0)^n \tilde{\phi}_{0n}^{(in)}(k_0, \infty)$ for $N = 9$, $k_0 = 0$, and the S-wave nucleon–nucleon potential (83). This corresponds to $N = 4$ in expansion (35). The closed curve shows the domain within which the exact Jost function is reproduced by this polynomial with the accuracy better than 1%. Cross indicates the position of the nucleon–nucleon virtual state (see table 2).

resonance is shifted to the point

$$k_0 = 2.5 - i0.01. \tag{84}$$

This was done by minimizing the value of $\left| \tilde{\phi}_{00}^{(in)}(k_0, \infty) \right|$ as a function of the two parameters H and w, which determine the shape of the barrier

$$V(r) = Hr^2 \exp(-wr). \tag{85}$$

The thus obtained values of its parameters, which put the resonance at the point (84), are

$$H = 6.673\,749\,255, \qquad w = 1.008\,562\,572.$$

7. Conclusions

Basically, in this paper the two things are done: first, we describe a systematic and accurate procedure for calculating any number of coefficients in the standard effective-range expansion, and second, we generalize this procedure in such a way that the expansion can be done not only around the threshold $k = 0$, but around an arbitrary point in the complex k-plane.

Using numerical examples, we demonstrate that the proposed method is stable and accurate. It enables us to obtain a polynomial approximation of the Jost function within a rather wide domain of the complex k-plane around a chosen point. In doing this, we obtain a Padé approximation of the S-matrix, which remains unitary by construction.

We show that the approximate Jost function can be used for locating resonances and virtual states. In addition to this, we describe a simple and accurate method for locating zero-energy bound states and a method for putting resonances at desired places of the k-plane by adjusting the potential.

It should be noted that in this paper we only consider short-range potentials. For the long-range interactions some modifications are needed because for them the wavefunction has different asymptotic behavior. Another class of problems that requires special treatment, constitute the multichannel problems. This, however, is beyond the scope of this paper.

References

[1] Bethe H A 1949 Theory of the effective range in nuclear scattering *Phys. Rev.* **76** 38-50
[2] Goldberger M L and Watson K M 1964 *Collision Theory* (New York: Wiley)
[3] Kynch G J 1952 *Proc. Phys. Soc.* A **65** 83 94
[4] Levy B R and Keller J B 1963 *J. Math. Phys.* **4** 54
[5] Dashen R F 1963 *J. Math. Phys.* **4** 338
[6] Babikov V V 1965 *Sov. J. Nucl. Phys.* **1** 793–802
[7] Babikov V V 1967 *Phys.—Usp.* **92** 3–26
[8] Pupyshev V V and Solovtsova O P 1992 *Int. J. Mod. Phys.* A **7** 2713
[9] Pupyshev V V and Rakityansky S A 1994 *Z. Phys.* A **348** 227
[10] Uang Y-H and Stwalley W C 1982 The possibility of a ^{4}He$_2$ bound state, effective range theory, and very low energy He–He scattering *J. Chem. Phys.* **76** 5069–72
[11] Buckman S J and Mitroy J 1989 Analysis of low-energy electron scattering cross sections via effective-range theory *J. Phys. B: At. Mol. Opt. Phys.* **22** 1365–84
[12] Marinescu M 1994 Computation of the scattering length and effective range in molecular physics *Phys. Rev.* A **50** 3177–80
[13] Arnecke F, Friedrich H and Madronero J 2006 Effective-range theory for quantum reflection amplitudes *Phys. Rev.* A **74** 062702
[14] Idziaszek Z and Karwasz G 2006 Applicability of modified effective-range theory to positron–atom and positron–molecule scattering *Phys. Rev.* A **73** 064701
[15] Idziaszek Z and Karwasz G 2007 Shape resonances in modified effective range theory for electron–molecule collisions arXiv:0708.2991 [physics.atom-ph]
[16] Brand L 1966 *Differential and Difference Equations* (New York: Wiley)
[17] Taylor J R 1972 *Scattering Theory* (New York: Wiley)
[18] Sofianos S A and Rakityansky S A 1997 *J. Phys. A: Math. Gen.* **30** 3725
[19] Abramowitz M and Stegun A (ed) 1964 *Handbook of Mathematical Functions* (Washington, DC: National Bureau of Standards)
[20] Rakityansky S A, Sofianos S A and Elander N 2007 *J. Phys. A: Math. Theor.* **40** 14857–69